Evaluating the Compressive Strength of Recycled Aggregate Concrete Using Novel Artificial Neural Network

Kennedy C. Onyelowe [1], Tammineni Gnananandarao [2], Ahmed M. Ebid [3*],
Hisham A. Mahdi [3], M. Razzaghian Ghadikolaee [4], Mohammed Al-Ajamee [5]

[1] Department of Civil and Mechanical Engineering, Kampala International University, Kampala, Uganda.

[2] Aditya College of Engineering and Technology, Aditya Nagar, Andhra Pradesh, India.

[3] Faculty of Engineering and Technology, Future University in Egypt, New Cairo 11865, Egypt.

[4] School of Civil Engineering, Iran University of Science and Technology, Tehran, Iran.

[5] Indian Institute of Technology, Guwahati, North Guwahati, Assam, India.

Abstract

In this work, the compressive strength of concrete made from recycled aggregate is studied and an intelligent prediction is proposed by using a novel artificial neural network (ANN), which utilizes a sigmoid function and enables the proposal of closed-form equations. An extensive literature search was conducted, which gave rise to 476 data points containing cement, sand, aggregates, recycled aggregates of fine to coarse texture, water, and plasticizer as the constituents of the concrete and the input variables of the intelligent model. The compressive strength (fc) of the recycled aggregate concrete (RAC), which was studied through multiple experiments, was the output variable of the model. The data points of concrete strength collected through literature show a consistent and sustained strength improvement with the increase in the recycled aggregate proportions. However, the outcome of the concrete compressive strength predictive model shows remarkable performance indices as follows; r is 0.99 and 0.99, R^2 is 0.98 and 0.97, MSE is 28.67% and 44.64%, RMSE is 5.35% and 6.68%, MAE is 4.12% and 5.01%, and MAPE is 12.73% and 13.83% for the model training and testing respectively. These results compared well with previous studies conducted on RAC with less data, different activation functions, and different techniques. Generally, the closed-form equation, which performed at an average accuracy of 97.5% with an internal consistency of 99%, has shown its potential to be applied in RAC design and construction activities for a sustainable performance evaluation of recycled aggregate concrete.

Keywords: Compressive Strength; Recycled Aggregate Concrete; Sustainable Construction; Eco-friendly Concrete.

1. Introduction

The construction industry and building materials account for 50% of the solid waste produced every year around the world [1]. According to the statistics for 2018, construction and demolition (C&D) waste reached approximately 3 billion tons over the world, which is around 50 percent of the total solid waste produced [2]. Hence, the utilization of the waste materials resulting from C&D has become an important priority. For nearly 70 years, studies have indicated that replacing natural aggregate (NA) with recycled aggregate (RA) from C&D in recycled aggregate concrete (RAC) production as a new generation of concrete can provide positive impacts on both the economy and the environment [3]
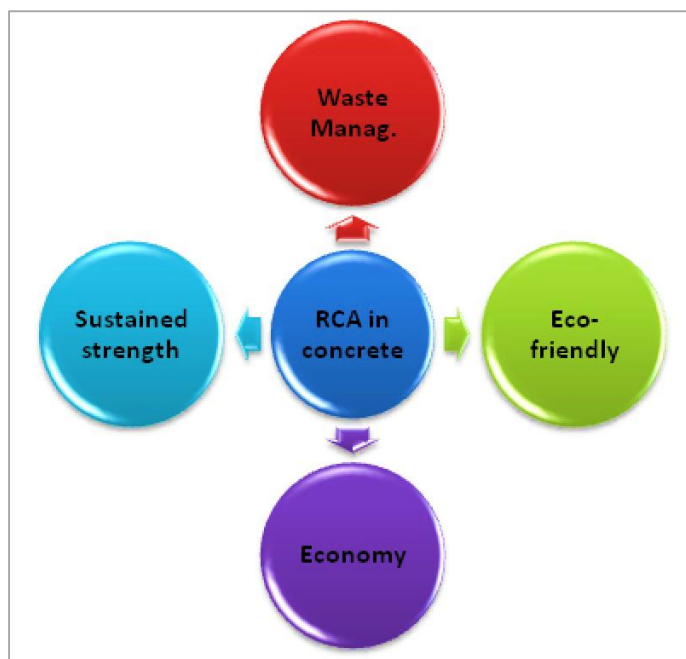
as presented in Figure 1. Indeed, C&D waste can be properly recycled and reused as coarse or fine aggregates instead of natural aggregates [4, 5]. It is estimated that the utilization of RA as a replacement for NA could save the cost of material by about 10-20% [6].

Figure 1. Structural, economic and environmental benefits of recycled aggregate in concrete

Although using RCA for making RAC is a positive step in the direction of sustainability, it has lower quality in terms of performance than concrete made with natural aggregates [7]. Accordingly, RAC exhibits low flexural, tensile, and compressive strength as well as high porosity, shrinkage, and water absorption [8-10]. Regarding many studies, the higher the replacement ratio of RA, the lower the flexural strength of RAC [11-15]. In accordance with the research performed by Bairagi et al. [11], RAC containing 25% and 50% recycled aggregates showed approximately 6-13% reduction in flexural strengths compared to that of the control sample. In addition to this procedure, replacing NA with 100% RA led to a 26% decrease in flexural strength. This phenomenon can be related to the poor interfacial bond between the new cement paste and the old cement paste covering RA [16]. Based on this reason, many methods have been applied throughout the years in order to ameliorate the flexural strength of recycled aggregate concrete, such as the utilization of nanomaterials, fibers, pozzolanic materials, etc.

Nowadays, nanotechnology has been developing, and nanomaterials have been mainly used in compounds with a number of conventional materials in order to ameliorate their characteristics [17-19]. Studies performed by Mukharjee et al. [20] have shown that the incorporation of nano-silica into the mix design of RAC can significantly make the microstructure denser due to its filling effect and pozzolanic activity; meanwhile, the flexural strength increased. Babar Ali et al. [21] reported that the compressive and flexural strength of RAC improves with the addition of proper dosage of glass fibers. They also found that the incorporation of 20% fly-ash as a replacement for cement results in better flexural strength for RAC in comparison to the normal concrete. The research conducted by Katkhuda et al. [22] showed that the optimum dosage of basalt fiber (0.3%) increased the compressive and flexural strengths of the RAC significantly. El Ouni et al. [23] discovered the proper dosage of polypropylene fiber (PPF) and steel fiber (SF) in terms of single or hybrid application (0.15%PPF-0.85%SF) can enhance the compressive and flexural strengths of RAC by around 26%. Yongggui et al. [24] reported that the simultaneous use of nano-silica and basalt fiber could ameliorate the flexural strength of RAC considerably. Shaban et al. [25] scrutinized the effect of pozzolan slurries on the properties of recycled aggregate concrete. Results indicated that RAC containing pozzolan has higher flexural strength compared to that of the untreated RAC due to higher pozzolanic reactivity. Indeed, the high pozzolanic activity enhances bonding between aggregate and matrix by reducing the pores in ITZ and the interlock among the aggregate and mortar compared with the control RAC. Moreover, the pozzolanic materials play a filler role in RAC, resulting in a decline of pores and voids volume in the adhered mortar. In general, the development of compressive and flexural strengths depends mainly on the bond strength between the concrete matrix and the aggregate [26]. This fact is assured by modifying RAC with pozzolan slurries, which ameliorates flexural strength development. These findings can probably be ascribed to the interaction between the pozzolan and $Ca(OH)_2$ existing in RCA during the hydration process, leading to the formation of additional C-S-H in the concrete matrix for reinforcing the bonding among the original aggregate and mortar. Hereupon, the mentioned technique ameliorates the flexural strength of RAC effectively [25].

Concrete is one of the world's most commonly used materials, and its manufacture requires significant natural resources each year. The availability of these natural resources is dwindling, which is a growing source of concern for the concrete industry. Long-term extraction of natural aggregates (NA) from lakes, riverbeds, and other water bodies has caused massive environmental concerns in several regions of the world [27, 28]. As a result, throughout the last few decades, researchers have attempted to incorporate various recycled materials in concrete. On the other hand, demolishing old structures produces a large volume of demolished concrete in landfills, causing major environmental issues such as landfill depletion. The recycling and reuse of demolished concrete by crushing it to obtain recycled concrete aggregate (RCA) to replace (NA) in natural aggregate concrete (NAC) has been given a high priority to conserve (NA) resources and limit discarded concrete [29, 30]. This approach complies with the international agenda to shift economic strategy from a linear to a cyclic one that is environmentally conscious. Such an approach could considerably enhance the management of non-renewable resources, resulting in a decrease in public landfills, reduced pollution, and lower construction costs [31].

Both coarse (RCA) and fine (RCA) produced after crushing demolished concrete to various sizes [32, 33], Due to large volume of attached mortar and old cement paste, which account for roughly 20–30% of the total volume in (RCA), the characteristics of (RCA) differ from those of (NA), resulting in increased water absorption and lower density of (RCA) compared to (NA).as consequence, the mechanical properties of recycled aggregate concrete (RAC) are different as compared to (NAC)with same mix proportions [34-38]. For coarse natural aggregate replacement (CNA), Rahal reported that the compressive strength of (RAC) was on the average 90% of those of (NAC) with the same mix proportions with 100% replacement [39]. However, Etxeberria et al [38]; concluded that (RAC) made with 100% replacement of (CRCA) has 20–25% less compression strength than (NAC), while (RAC) made with 25% of (CRCA) has same mechanical properties of (NAC) [38]. Nevertheless, for fine natural aggregate replacement (FNA), the compressive strength of (RAC) is not affected by fine aggregate replacement ratios up to 30% [40], while 15% and 30% reduction were reported by Khatib [41] for 25 % and 100% replacement level respectively. In addition, for both (CRCA) and (FRCA) replacement, 30% reduction of compressive strength of (RAC) for 100% replacement level was recorded. However, mechanical properties improved by incorporating silica fume and/or using plasticizer [42]. Compressive strength of (RAC) varies considerably for type of replacement, presence of plasticizers, water and cement content [32, 40, 42].

It can be seen from the above literatures that the compressive strength of (RAC) is in general inferior to compressive strength of (NAC). Several regression models have been developed to predict the compressive strength of (RAC), based on mix proportions such as Cabral et al. and Lovato et al. models [43, 44]; or based on reference (NAC) compressive strength such as Younis & Pilakoutas model [45]. However, due to disperse behaviour of (RAC), predicting Compressive strength using traditional methods is complicated and inaccurate [46]. Furthermore, because data from outside the project is more plentiful and continues to expand in volume and complexity in comparison to data acquired from the project of interest, relying just on human judgment isn't deemed to be a viable approach. This raises the question of how to supplement current empiricism-based practice with data-driven methodologies to get the most value out of data for decision-making. Given that engineering judgment is still important in decision-making, it is useless when dealing with the volume, variety, velocity, and veracity of such big data [47]. Recently, Artificial intelligence techniques have proven to be effective in providing end users with fairly accurate insights on concrete mechanical properties [48]. Therefore, predictive models based on artificial intelligence methods have been used to predict compressive strength of (RAC) and the effect of mix proportions on its behavior [48, 49-54]. In this research paper, a sigmoid activation function has been employed in the intelligent abilities of the ANN to predict the fc of a multiple database for a recycled aggregate concrete (RAC) and propose a closed-form equation for the studied concrete property.

Artificial neural networks are a mathematically simulated system that may be constructed in a computer and replicate the human brain's neural network system. The current opinion of ANNs is that they are capable of imitating natural insight in their learning from experience [55]. An ANN is made up of a series of processing elements, such as nodes or neurons that are organised in layers such as input, output, and one or more hidden layers between them. ANN and similar soft computing techniques are usually utilized to find the relationship or program between input and output variables. ANN, unlike traditional methods, can produce acceptable results in less time and without the need of pre-defined criteria, assumptions, or rules. At the ANN process, inputs are adapted in the hidden layer and then turned into network results after exiting the output layer. On the training data, ANN utilises a learning rule to find a set of weights. Then, the network generates fresh output with a high level of precision. Thereafter, additional data set is required to confirm the training phase's performance. This procedure is repeated till the error is reduced to a minimum [56].

The multilayer perceptron (MLP) is one of the most extensively used feed-forward architecture of ANN model structures. Rumelhart & McClelland [57] and McClelland & Rumelhart [58] methods for training MLP, the back propagation (BP) or backward propagation of errors technique was devised. Each layer's neuron is connected to all neurons in the next layer via weighted connections in MLP. However, each layer can carry out its own calculations on receiving data from the preceding layer. In the ANN, an adaptive weight coefficient (η_{ij}) connects two layers and multiplies each input (x) from the preceding layer. Then, the weighted inputs are then combined together (Summation Function) and a bias value (ξ_j) is added. The ANN's output layer (y) or the input of the following layer is then produced

by a function (Transfer Function). The sigmoid function is commonly used as transfer function for nonlinear issues [56, 59, 60]. The below Equation 1 usually depicts this process.

$$y_j = f\left(\sum_{i=1}^{n} \eta_{ij} \times x_i + \xi_j\right)$$ (1)

By propagating errors from the output to the input, the BP method modifies network weights. To minimise the error, the process was reversed and the weight values were adjusted in this algorithm [56, 59]. The following Equation 2 (error function (E_f)) can be reduced by changing the inter-connections between layers:

$$E_f = \frac{1}{2}\sum_{n}\sum_{k}\left(C_k^n - A_k^n\right)^2$$ (2)

where, C_k^n is the calculated output; A_k^n is the actual output value; n is the number of samples; and k is the number of output neurons.

2. Methodology

2.1. Data Collection

ANN model is developed using the extensive compiled data of 476 obtained from the regressive experimentation of previous literatures [32-54]. The data consists of eight input parameters and one output parameter. The varied parameters are cement content (C) ton/m^3, sand content (S) ton/m^3, recycled fine aggregate content (FAr) tom/m^3, coarse aggregates content (CA) tom/m^3, recycled coarse aggregates content (CAr) ton/m^3, water content (W) ton/m^3, plasticizers content (P) ton/m^3, compressive strength of concrete (f'c) MPa corresponding to 28 days. For way of creating modelling, the experimental findings were chosen at random for training and testing. It is essential to assess the neural network model's generalisation capability using the data set of testing. Because the variables are continuous, changing the percentage of training and testing data sets has no effect on the model. Further, 70% of the total records were taken for training, with the remaining 30% being utilised to test the model. The methodology flowchart of the research paper is presented on Figure 2.
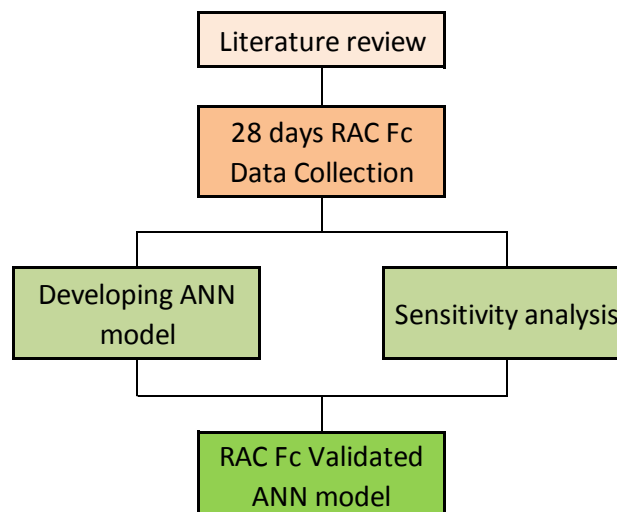

Figure 2. Methodology flowchart of the research work

2.2. Preparation of ANN's Model

The selection of the architecture (input-hidden-output layer's) for the ANN's model is the most important step followed by the number of iterations. In the present study, eight independent parameters are selected as input neurons and one output neuron for the input layer and output layer. To finalize the hidden layer neurons, the ANN model was run by varying the hidden layer neurons and corresponding coefficient of determination (R^2) and the mean square error (MSE) are calculated and the variation is shown in Figure 3. From Figure 3, where the R^2 is high and MSE is low, corresponding point is located as optimum hidden neurons and the same was highlighted in the Figure 3. However, over fitting is the major problem in simplification of ANN model as it depends on the epochs/iterations. Hence, to overcome this over fitting (which leads to poor prediction), the optimum epochs were fixed by calculating the MSE for each lift of the epoch (each lift is 10). The lowest MSE/no increment or decrement in the MSE corresponding epochs were selected as an optimum epoch number for this model based on Dutta et al. [61], Gnananandarao et al. [62], and Onyelowe et al. [63]. The variation of epochs and MSE are shown in Figure 4 and from there, the number of epochs were fixed by following the above procedural steps. Finally, the number of iterations was fixed as 4500 and the structure of present study constitutive ANN model is 8-7-1. The structure of the ANN model is shown in Figure 5.
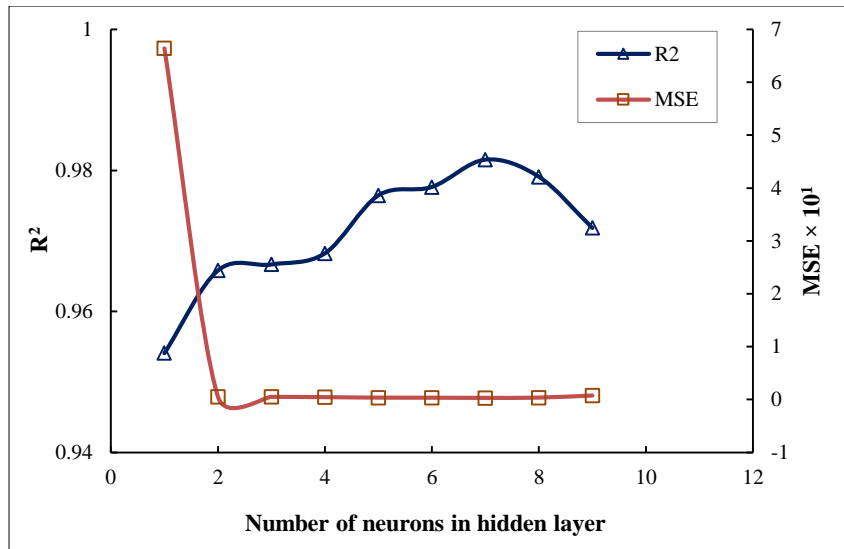
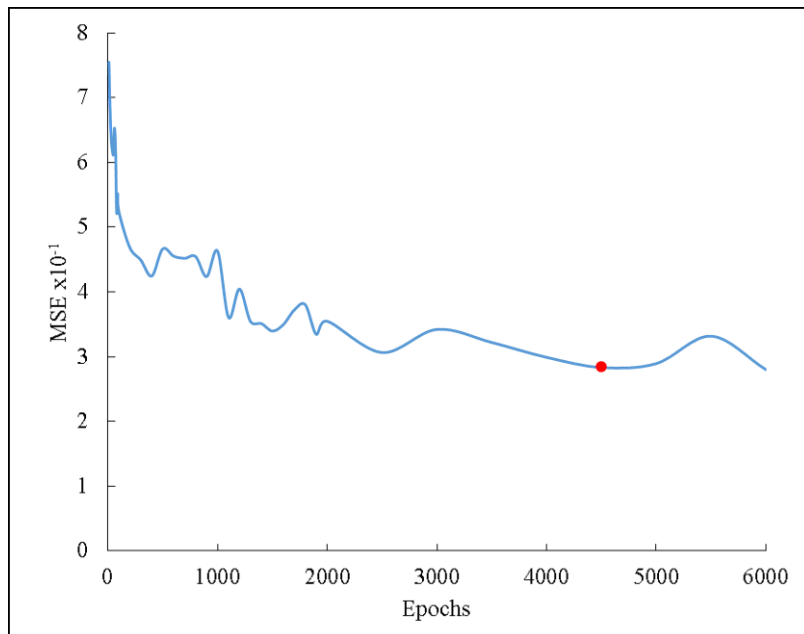**Figure 3. Variation plot among the R^2, MSE and hidden layer neurons**

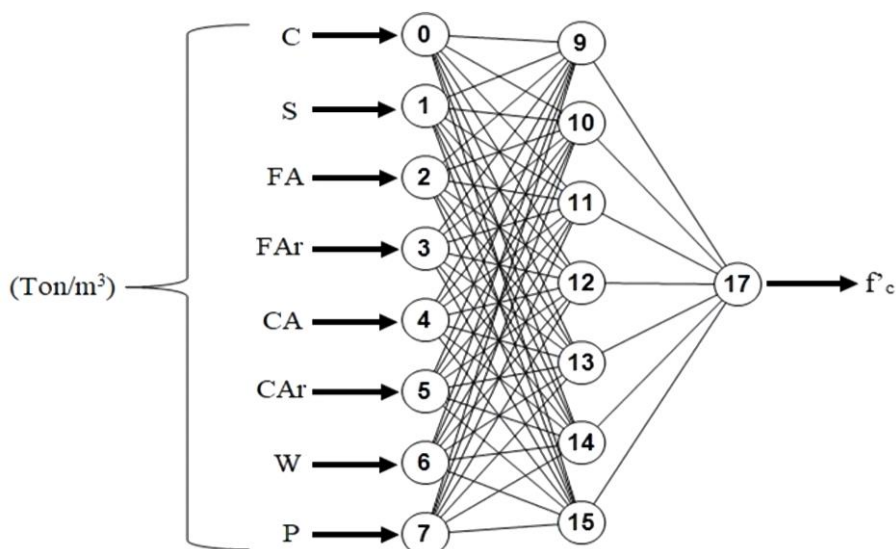

Figure 4. Variation of MSE versus epochs

Figure 5. Structure of the ANN model for compressive strength of concrete

2.3. Selection of Activation Function

The activation function in the ANN determines whether or not a neuron should be stimulated by computing a weighted sum and then adding bias to it. The aim of the activation function is to establish non-linearity into a neuron's output. However, the neurons in a neural network work in accordance with their weight, bias, and activation function [63]. The weights and biases of the neurons in a neural network would be updated based on the output error and it is called Back-propagation. The activation functions can enable back-propagation since the gradients are provided simultaneously with the errors to update the weights and biases [62, 63]. Without an activation function, a neural network will essentially become a linear regression model. The activation function transforms the input in a non-linear procedure, allowing it to learn and accomplish more complex tasks. A total of 18 activation functions were used in this research work and same functions were shown in Table 2. The open-source AgielNN software supports these functions. The predicted compressive strength of recycled aggregate concrete for both the training and testing data sets is identical to the targeted compressive strength of the concrete after 4500 iterations.

2.4. Performance Measures

After the model has been identified, it was tested for its ability to forecast concrete compressive strength using both predicted and measured data. In the present study, six statistics parameters were used (r, R^2, MSE, RMSE, MAE and MAPE). The full name of each statistical parameter with mathematical expression is presented in the Table 1. The r & R^2 calculated values are close to 1 and the MSE, RMSE, MAE & MAPE are minimum and considered to be a good prediction of the desired output. However, readers can refer to the literature [64-66] for more details about performance measure. The calculated values of all the six parameters for different activation function is presented in Table 2 for both training and testing. From the Table 2, it can be concluded that the best activation function is sigmoid followed by sigmoid stepwise. Hence, sigmoid activation function (weights and biases) is used for further execute the development of model equation and sensitivity analysis in the future sections.

Table 1. Mathematical expression of statistical coefficients

Statistical coefficient	Mathematical expression
Correlation coefficient (r)	$r = \dfrac{\sum f'_{c_{ht}} \times f'_{c_{hp}} - n \overline{f'_{c_{ht}}} \times \overline{f'_{c_{hp}}}}{(n-1) S_{f'_{c_{ht}}} S_{f'_{c_{hp}}}}$
Coefficient of determination (R^2)	$R^2 = 1 - \dfrac{\sum_i (f'_{c_{hp}} - f'_{c_{ht}})^2}{\sum_i (f'_{c_{hp}} - \overline{f'_{c_{hp}}})^2}$
Mean square error (MSE)	$MSE = \dfrac{1}{n} \sum_{i=1}^{n} (f'_{c_{ht}} - f'_{c_{hp}})^2$
Root mean square error (RMSE)	$RMSE = \sqrt{\dfrac{1}{n} \sum_{i=1}^{n} (f'_{c_{ht}} - f'_{c_{hp}})^2}$
Mean absolute error (MAE)	$MAE = \dfrac{1}{n} \sum_{i=1}^{n} \left| f'_{c_{ht}} - f'_{c_{hp}} \right|$
Mean absolute percentage error (MAPE)	$MAPE = \left[\dfrac{1}{n} \sum_{i=1}^{n} \left| \dfrac{f'_{c_{ht}} - f'_{c_{hp}}}{f'_{c_{ht}}} \right| \right] \times 100$

Note: $\acute{f}_{c_{ht}}, \acute{f}_{c_{hp}}$ target and predicted compressive strength of concrete, $\overline{f}_{c_{ht}}, \overline{f}_{c_{hp}}$:mean of the target and predicted compressive strength of concrete respectively, $S_{\acute{f}_{c_{ht}}}, S_{\acute{f}_{c_{hp}}}$:standard deviation of the target and predicted compressive strength of concrete respectively, n: number of observations

Table 2. Calculated results of performance measures for different activation functions

Activation function	Training						Testing					
	r	R^2	MSE	RMSE	MAE	MAPE	r	R^2	MSE	RMSE	MAE	MAPE
Cos	0.96	0.90	131.10	11.45	8.03	23.07	0.96	0.89	141.45	11.89	8.27	22.00
Cos symmetric	0.98	0.95	75.68	8.70	6.93	21.29	0.98	0.94	86.03	9.28	7.71	21.78
Elliot	0.99	0.98	35.78	5.98	4.55	14.08	0.99	0.96	56.52	7.52	5.73	15.60
Elliot symmetric	0.98	0.94	81.17	9.01	6.72	19.54	0.98	0.94	84.16	9.17	6.85	18.03
Gaussian	0.99	0.98	32.77	5.72	4.36	13.69	0.99	0.97	45.17	6.72	5.18	14.38
Gaussian symmetric	0.97	0.94	98.57	9.93	8.09	25.40	0.96	-2.84	751.82	27.42	24.27	59.28
Gaussian stepwise	0.95	-2.40	666.38	25.81	22.74	57.66	0.97	0.94	108.98	10.44	8.75	25.26
Linear	0.98	0.95	69.93	8.36	6.40	19.35	0.98	0.95	71.94	8.48	6.68	18.38
Linear Piece	0.97	0.93	118.15	10.87	8.85	29.56	0.97	0.92	126.6	11.25	9.12	28.27
Linear piece symmetric	0.98	0.95	69.52	8.34	6.26	19.04	0.99	0.96	67.45	8.21	6.38	17.72
<u>Sigmoid</u>	<u>0.99</u>	<u>0.98</u>	<u>28.67</u>	<u>5.35</u>	<u>4.12</u>	<u>12.73</u>	<u>0.99</u>	<u>0.97</u>	<u>44.64</u>	<u>6.68</u>	<u>5.01</u>	<u>13.83</u>
Sigmoid stepwise	0.99	0.98	32.86	5.73	4.40	13.24	0.99	0.96	51.51	7.18	5.53	14.89
Sigmoid symmetric	0.98	0.95	78.24	8.85	6.85	20.49	0.98	0.94	81.88	9.05	7.24	19.66
Sigmoid symmetric stepwise	0.98	0.96	65.58	8.10	6.18	19.37	0.99	0.96	69.13	8.31	6.57	18.78
Sin	0.98	0.95	63.49	7.97	6.08	17.80	0.98	0.93	93.11	9.65	6.85	17.69
Sin symmetric	0.98	0.95	68.01	8.25	6.26	19.15	0.98	0.95	74.04	8.60	6.65	18.21
Threshold	0.99	0.98	32.86	5.73	4.40	13.24	0.80	-92.53	272746	522.2	385.1	75.04
Threshold Symmetric	0.58	0.34	3354.4	57.92	53.04	167.68	0.53	0.28	3521.9	59.35	53.68	163.32

2.5. Model Equation

Following the proposed architecture 8-7-1 as shown in the Figure 5 and the optimum iterations of 4500, the model was executed and the prediction results of compressive strength of concrete were validated with the performance measures. The best activation function was selected and the same model weights gap between the input and hidden layers; the gap in weights between hidden and output layer; bias at the layer of input; and bias at the layer of output were represented in terms of matrix $[\eta_{ji}]$, $[\chi_{jk}]$, $[\xi_j]$, $[\xi_0]$, respectively and simultaneously showed in the Equations 3 to 6, respectively. In the above-represented matrices, η_{ji} is the weight between i_{th} neuron in input layer and j_{th} neuron in hidden layer. χ_{jk} is the weight between j_{th} neuron in hidden layer and k_{th} neuron in output layer. ξ_j is the bias at j_{th} neuron in hidden layer and ξ_0 is the bias at output layer.

$$
\eta_{ji} = \begin{bmatrix}
\eta_{11} & \eta_{12} & \eta_{13} & \eta_{14} & \eta_{15} & \eta_{16} & \eta_{17} & \eta_{18} \\
\eta_{21} & \eta_{22} & \eta_{23} & \eta_{24} & \eta_{25} & \eta_{26} & \eta_{27} & \eta_{28} \\
\eta_{31} & \eta_{32} & \eta_{33} & \eta_{34} & \eta_{35} & \eta_{36} & \eta_{37} & \eta_{38} \\
\eta_{41} & \eta_{42} & \eta_{43} & \eta_{44} & \eta_{45} & \eta_{46} & \eta_{47} & \eta_{48} \\
\eta_{51} & \eta_{52} & \eta_{53} & \eta_{54} & \eta_{55} & \eta_{56} & \eta_{57} & \eta_{58} \\
\eta_{61} & \eta_{62} & \eta_{62} & \eta_{63} & \eta_{64} & \eta_{65} & \eta_{66} & \eta_{67} \\
\eta_{71} & \eta_{72} & \eta_{73} & \eta_{74} & \eta_{75} & \eta_{76} & \eta_{77} & \eta_{78}
\end{bmatrix} = \begin{bmatrix}
-11.28 & -34.46 & 14.63 & 18.48 & 5.79 & 4.48 & -9.50 & -4.54 \\
0.08 & -9.40 & -4.88 & -0.95 & 3.43 & -5.57 & -6.24 & 3.49 \\
-3.46 & 5.99 & 6.60 & 6.08 & 8.53 & 9.52 & -1.61 & 3.22 \\
-13.00 & 8.77 & -5.50 & 0.17 & -5.66 & -3.97 & 0.82 & -10.09 \\
1.89 & 9.64 & -1.20 & 5.84 & -1.04 & -1.33 & -10.77 & -3.85 \\
-8.75 & -9.03 & -3.10 & 3.75 & -3.41 & -9.10 & -5.23 & -5.08 \\
-10.92 & 7.14 & -7.68 & -4.98 & -3.12 & -0.96 & 2.43 & -1.80
\end{bmatrix} \tag{3}
$$

$$
\chi_{jk} = \begin{bmatrix}
\chi_{11} \\ \chi_{21} \\ \chi_{31} \\ \chi_{41} \\ \chi_{51} \\ \chi_{61} \\ \chi_{71}
\end{bmatrix} = \begin{bmatrix}
8.52 \\ 3.18 \\ -5.13 \\ -1.35 \\ 2.21 \\ -2.16 \\ -1.71
\end{bmatrix} \tag{4}
$$

$$
\xi_j = \begin{bmatrix}
\xi_1 \\ \xi_2 \\ \xi_3 \\ \xi_4 \\ \xi_5 \\ \xi_6 \\ \xi_7
\end{bmatrix} = \begin{bmatrix}
-12.91 \\ 2.56 \\ -13.48 \\ 0.45 \\ -4.03 \\ 10.75 \\ -4.90
\end{bmatrix} \tag{5}
$$

$$\xi_0 = [-0.54] \tag{6}$$

Further, the weights & biases as presented in the Equations 3 to 6 were used to develop the ANN's model equation as followed by the basic Equation 7 [67].

$$f'_c = f_n \left\{ \xi_0 + \sum_{j=1}^{h} \left[\eta_{jk} f_n \left(\sum_{i=1}^{n} \chi_{jk} X_i \right) \right] \right\} \tag{7}$$

where, h is number of neurons in hidden layer = 7, n are the number of neurons in input layer = 8 and X_i is the normalized value of inputs.

The steps required to develop model equation include calculation of A1–A6 and b1–b6 using Equations 8 to 13 and Equations 14 to 19, respectively. The final expression takes the form as Equation 20 which is the normalized output, the de-normalized forms of which are represented by Equations 21 and 22.

$$A_1 = \eta_{11} \times C + \eta_{12} \times S + \eta_{13} \times FA + \eta_{14} \times FAr + \eta_{15} \times CA + \eta_{16} \times CAr + x_{17} \times W + \eta_{18} \times P \tag{8}$$

$$A_2 = \eta_{21} \times C + \eta_{22} \times S + \eta_{23} \times FA + \eta_{24} \times FAr + \eta_{25} \times CA + \eta_{26} \times CAr + x_{27} \times W + \eta_{28} \times P \tag{9}$$

$$A_3 = \eta_{31} \times C + \eta_{32} \times S + \eta_{33} \times FA + \eta_{34} \times FAr + \eta_{35} \times CA + \eta_{36} \times CAr + x_{37} \times W + \eta_{38} \times P \tag{10}$$

$$A_4 = \eta_{41} \times C + \eta_{42} \times S + \eta_{43} \times FA + \eta_{44} \times FAr + \eta_{45} \times CA + \eta_{46} \times CAr + x_{47} \times W + \eta_{48} \times P \tag{11}$$

$$A_5 = \eta_{51} \times C + \eta_{52} \times S + \eta_{53} \times FA + \eta_{54} \times FAr + \eta_{55} \times CA + \eta_{56} \times CAr + x_{57} \times W + \eta_{58} \times P \tag{12}$$

$$A_6 = \eta_{61} \times C + \eta_{62} \times S + \eta_{63} \times FA + \eta_{64} \times FAr + \eta_{65} \times CA + \eta_{66} \times CAr + x_{67} \times W + \eta_{68} \times P \tag{13}$$

$$b_1 = \frac{1}{1 + e^{-A_1}} \tag{14}$$

$$b_2 = \frac{1}{1 + e^{-A_2}} \tag{15}$$

$$b_3 = \frac{1}{1 + e^{-A_3}} \tag{16}$$

$$b_4 = \frac{1}{1 + e^{-A_4}} \tag{17}$$

$$b_5 = \frac{1}{1 + e^{-A_5}} \tag{18}$$

$$b_6 = \frac{1}{1 + e^{-A_6}} \tag{19}$$

$$B_1 = b_1 + b_2 + b_3 + b_4 + b_5 + b_6 + \xi_0 \tag{20}$$

$$f'_{c_{be-denormal}} = \frac{1}{1 + e^{-B_1}} \tag{21}$$

After de-normalization

$$f'_{c_{de-normal}} = 0.5 \left(f'_c + 1 \right) \left(f'_{c_{max}} - f'_{c_{min}} \right) + f'_{c_{min}} \tag{22}$$

3. Results and Discussions

3.1. General Outcome

The ANN model for the best activation function (sigmoid) to predict the compressive strength of concrete was developed. The model gives $R^2 > 0.8$ and error parameter values (MSE, RMSW, and MAPE) are minimums; these indicate that the proposed model has strong correlation agreement between the estimated and measured values as per

Smith [68]. To see the agreement between the predicted and measured values, the graphs are drawn for the training and testing as shown in Figures 6 and 7, respectively. The study of the Figures 6 and 7 show that the R^2 values are 0.98 and 0.97 for training and testing, respectively. It concludes that, the model is good in predicting the compressive strength of concrete. From further study of the Figures 6 and 7, it can be revealed that the values are within the $\pm$ 15 % region from the line of equality. Finally, a plot is drawn for the testing data to see the variation of the ANNs models and the experimental data and is shown in Figure 8. It reveals that the predicted ANN model values are closely fitting with the experimental data. From Figures 6 to 8, it can be concluded that the proposed ANN model can predict the compressive strength of concrete in precise manner.
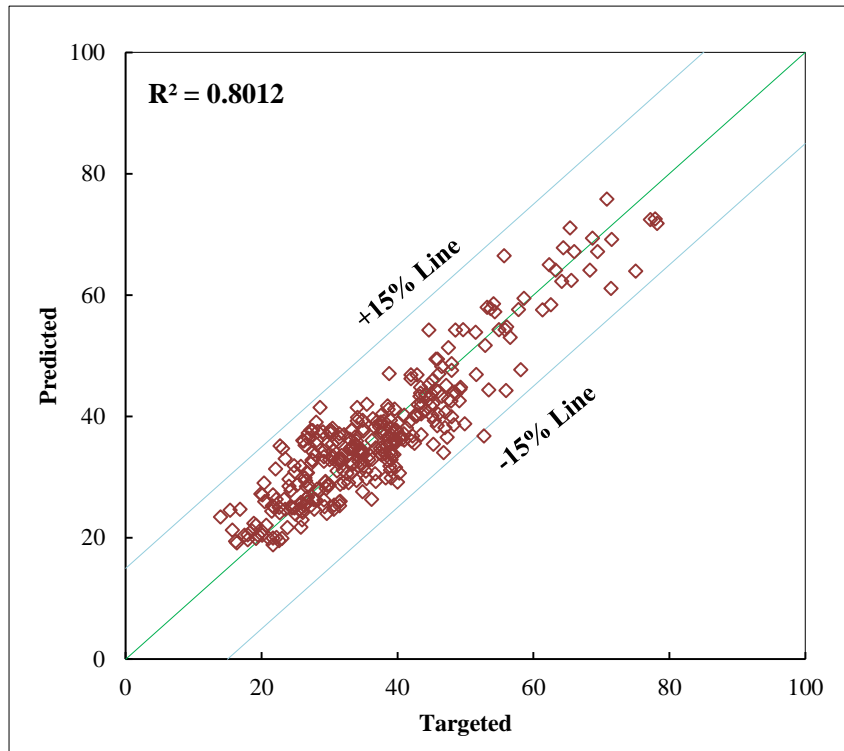

Figure 6. Illustration of variation for the targeted & predicted ANN trained compressive strength of concrete data
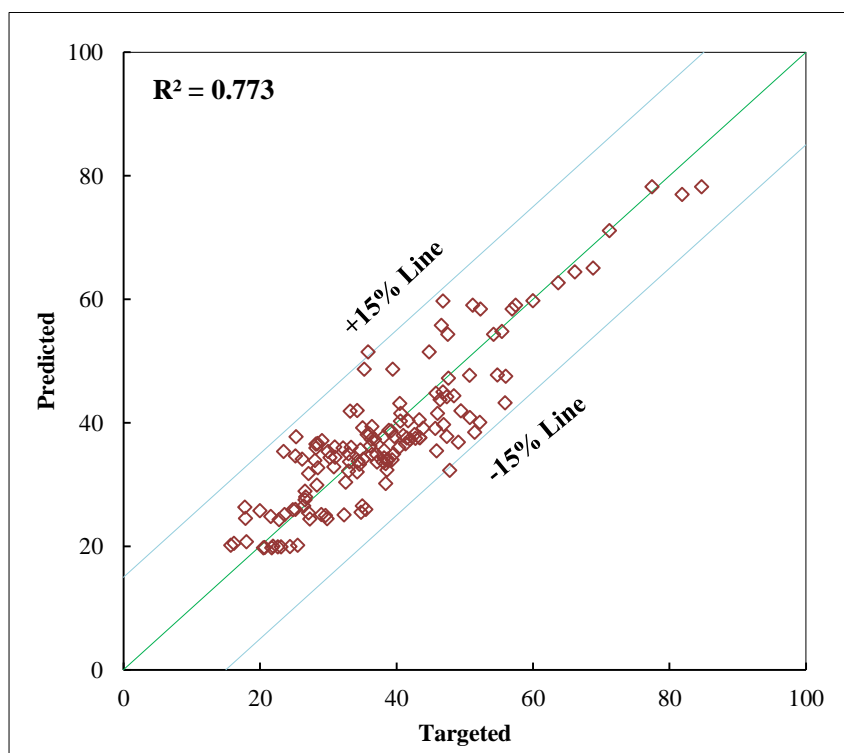

Figure 7. Illustration of variation for the targeted & predicted ANN tested compressive strength of concrete data
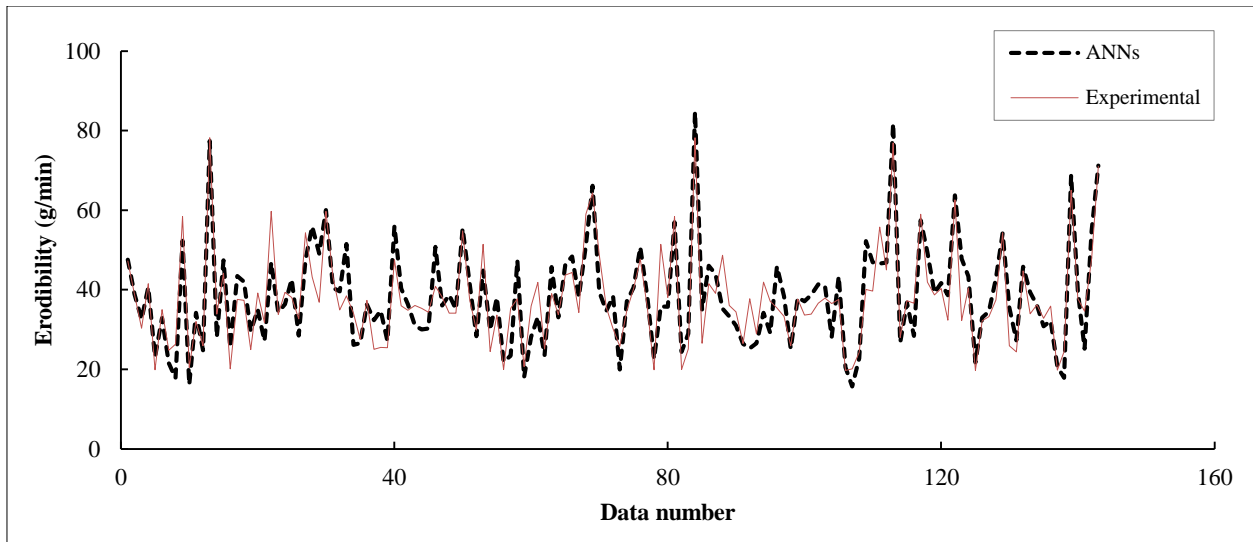
Figure 8. Variation comparison of the experimental and ANNs tested data for compressive strength of concrete

3.2. Sensitivity Analysis

The sensitivity analysis is used in this section of the study to discuss the impact of individual input variables on the compressive strength of concrete (output). The methods (based on the weight and bias) reported by Garson [69] and Olden and Jackson [70] were used for this purpose. In the technique proposed by Garson [69], each hidden neuron's weight values in the hidden layer were separated into components. Every input neuron had all these components connected to it. The determined individual influence value is shown in Figure 9 as a pie chart. In the next technique proposed by Olden and Jackson [70] for all input neurons, the total of the final weights of the connections (input to hidden neurons and hidden to output neurons) is determined. The impact of each individual variable on a given input is calculated using the approach described in the Garson [69] and Olden and Jackson [70] literature. The findings from the results are shown in Figure 10. Further, from Figures 9 and 10, it may be concluded in both Garson [69] and Olden and Jackson [70] cases that, sand content (S) ton/m^3; water content (W) ton/m^3; and plasticizers content (P) ton/m^3 togethercontribute 61% and 62% respectively. In both methods, the major contributor is sand content (S) ton/m^3. The second major contributor is recycled fine aggregate content (FAr) tom/m^3 in the Garson [69] method and water content (W) ton/m^3 in the Olden and Jackson [70] method. The third major contributor is water content (W) ton/m^3 in the Garson [69] method and recycled fine aggregate content (FAr) in the Olden & Jackson [70] method. Remaining parameters influence the out by ±10% individually.
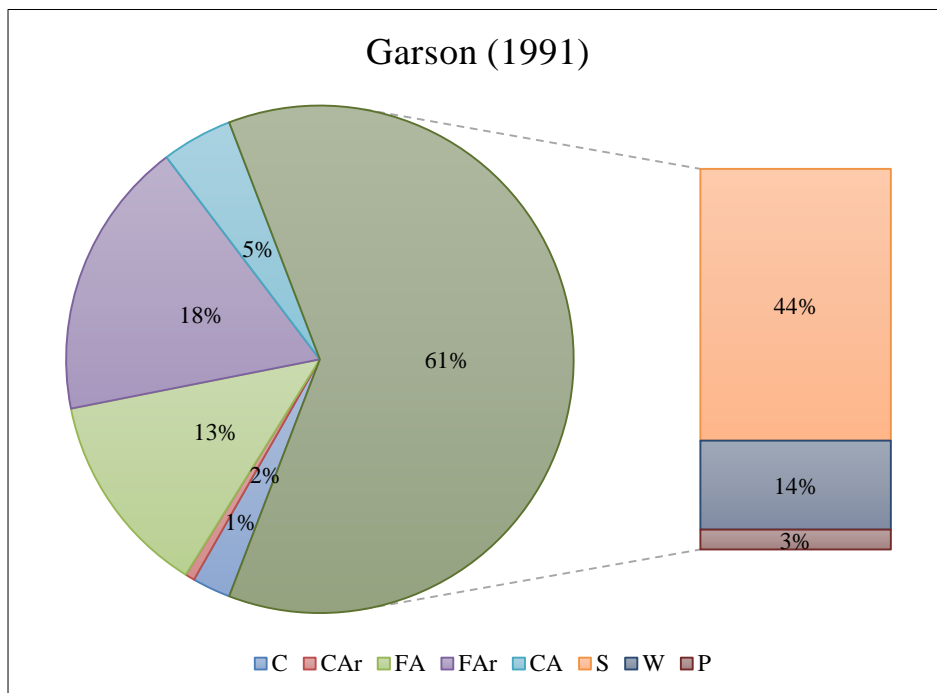

Figure 9. Relative importance of input variables on compressive strength of concrete
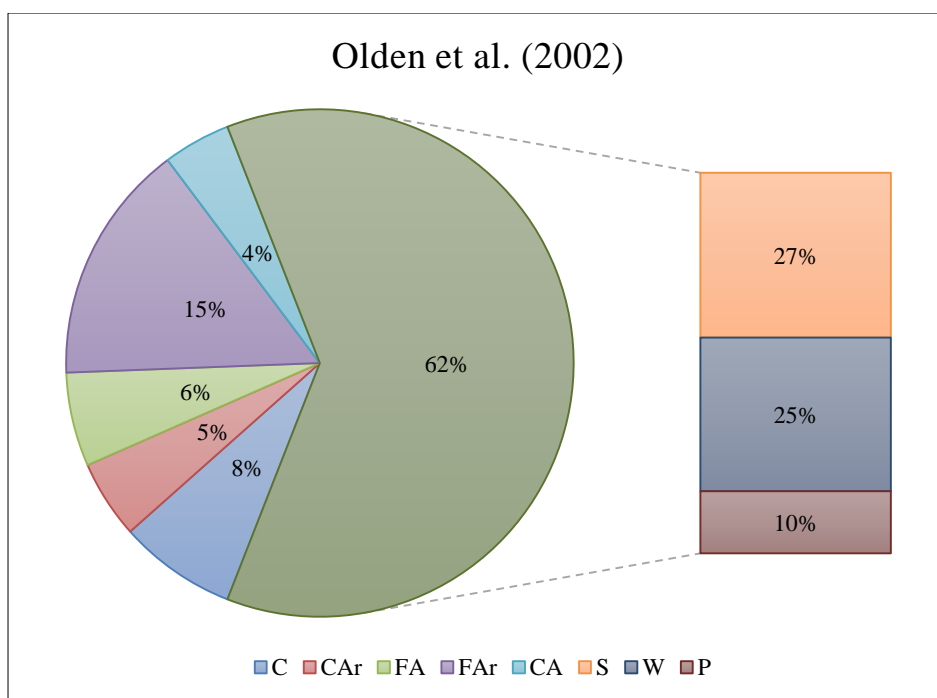
Figure 10. Relative importance of input variables on compressive strength of concrete

4. Conclusions

From the foregoing model exercise on the compressive strength of recycled aggregate concrete, the following can be concluded:

- For predicting the compressive strength of concrete mixed with recycled aggregate using the ANN model, the optimum architecture and iteration are 8-7-1 and 4500, respectively;

- The best activation functions for the predation of the compressive strength of the recycled aggregate concrete using the ANN model is sigmoid;

- From the sensitivity analysis, sand content (S) ton/m^3, water content (W) ton/m^3 and plasticizers content (P) ton/m^{3}contribute 61% and 62%, respectively, in order to predict the compressive strength of concrete;

- Based on the overall performance of the proposed ANN model, it can be concluded that the proposed model can predict the compressive strength of any recycled aggregate concrete in precise manner.

5. Declarations

5.1. Author Contributions

Conceptualization, K.C.O.; methodology, A.M.E.; software, M.A.; formal analysis, M.R.G.; investigation, T.G.; supervision, H.A.M. All authors have read and agreed to the published version of the manuscript.

5.2. Data Availability Statement

The data presented in this study are available in the article.

5.3. Funding

The authors received no financial support for the research, authorship, and/or publication of this article.

5.4. Conflicts of Interest

The authors declare no conflict of interest.

6. References

[1] Jain, M. S. (2021). A mini review on generation, handling, and initiatives to tackle construction and demolition waste in India. Environmental Technology and Innovation, 22. doi:10.1016/j.eti.2021.101490.

[2] Akhtar, A., & Sarmah, A. K. (2018). Construction and demolition waste generation and properties of recycled aggregate concrete: A global perspective. Journal of Cleaner Production, 186, 262–281. doi:10.1016/j.jclepro.2018.03.085.

[3] Naouaoui, K., & Cherradi, T. (2021). A case study on the mechanical and durability properties of a concrete using recycled aggregates. Civil Engineering Journal, 7(11), 1909-1917. doi:10.28991/cej-2021-03091768.

[4] Muduli, R., & Mukharjee, B. B. (2020). Performance assessment of concrete incorporating recycled coarse aggregates and metakaolin: A systematic approach. Construction and Building Materials, 233, 117223. doi:10.1016/j.conbuildmat.2019.117223.

[5] Younis, K. H., & Mustafa, S. M. (2018). Feasibility of Using Nanoparticles of SiO2 to Improve the Performance of Recycled Aggregate Concrete. Advances in Materials Science and Engineering, 2018. doi:10.1155/2018/1512830.

[6] Zheng, L., Wu, H., Zhang, H., Duan, H., Wang, J., Jiang, W., Dong, B., Liu, G., Zuo, J., & Song, Q. (2017). Characterizing the generation and flows of construction and demolition waste in China. Construction and Building Materials, 136, 405–413. doi:10.1016/j.conbuildmat.2017.01.055.

[7] Vázquez, V. F., Terán, F., & Paje, S. E. (2020). Dynamic stiffness of road pavements: Construction characteristics-based model and influence on tire/road noise. Science of the Total Environment, 736, 139597. doi:10.1016/j.scitotenv.2020.139597.

[8] Zhan, P. min, Zhang, X. xiang, He, Z. hai, Shi, J. yan, Gencel, O., Hai Yen, N. T., & Wang, G. cai. (2022). Strength, microstructure and nanomechanical properties of recycled aggregate concrete containing waste glass powder and steel slag powder. Journal of Cleaner Production, 341, 130892. doi:10.1016/j.jclepro.2022.130892.

[9] Neves, R., & de Brito, J. (2022). Estimated service life of ordinary and high-performance reinforced recycled aggregate concrete. Journal of Building Engineering, 46, 103769. doi:10.1016/j.jobe.2021.103769.

[10] Kazmi, S. M. S., Munir, M. J., & Wu, Y. F. (2021). Recycled aggregate concrete: Mechanical and durability performance. Handbook of Sustainable Concrete and Industrial Waste Management, 211–227, Woodhead Publishing, Sawston, United Kingdom. doi:10.1016/B978-0-12-821730-6.00017-6.

[11] Bairagi, N. K., Ravande, K., & Pareek, V. K. (1993). Behaviour of concrete with different proportions of natural and recycled aggregates. Resources, Conservation and Recycling, 9(1–2), 109–126. doi:10.1016/0921-3449(93)90036-F.

[12] Padmini, A. K., Ramamurthy, K., & Mathews, M. S. (2009). Influence of parent concrete on the properties of recycled aggregate concrete. Construction and Building Materials, 23(2), 829–836. doi:10.1016/j.conbuildmat.2008.03.006.

[13] Katz, A. (2003). Properties of concrete made with recycled aggregate from partially hydrated old concrete. Cement and Concrete Research, 33(5), 703–711. doi:10.1016/S0008-8846(02)01033-5.

[14] Malešev, M., Radonjanin, V., & Marinković, S. (2010). Recycled concrete as aggregate for structural concrete production. Sustainability, 2(5), 1204–1225. doi:10.3390/su2051204.

[15] Topçu, İ. B., & Şengel, S. (2004). Properties of concretes produced with waste concrete aggregate. Cement and Concrete Research, 34(8), 1307–1312. doi:10.1016/j.cemconres.2003.12.019.

[16] Onyelowe, K. C., Kontoni, D.-P. N., Ebid, A. M., Dabbaghi, F., Soleymani, A., Jahangir, H., & Nehdi, M. L. (2022). Multi-Objective Optimization of Sustainable Concrete Containing Fly Ash Based on Environmental and Mechanical Considerations. Buildings, 12(7), 948. doi:10.3390/buildings12070948.

[17] Razzaghian Ghadikolaee, M., Habibnejad Korayem, A., Sharif, A., & Ming Liu, Y. (2021). The halloysite nanotube effects on workability, mechanical properties, permeability and microstructure of cementitious mortar. Construction and Building Materials, 267, 120873. doi:10.1016/j.conbuildmat.2020.120873.

[18] Razzaghian Ghadikolaee, M., Habibnejad Korayem, A., Ghoroqi, M., & Sharif, A. Effect of halloysite nanotubes on workability and permeability of cement mortar. Modares Civil Engineering Journal, 18(2), 89–100.

[19] Razzaghian Ghadikolaee, M., Mirzaei, M., & Habibnejad Korayem, A. (2021). Simultaneous effects of nanosilica and basalt fiber on mechanical properties and durability of cementitious mortar: an experimental study. Canadian journal of civil engineering, 48(10), 1323-1334. doi:10.1139/cjce-2020-0129.

[20] Mukharjee, B. B., & Barai, S. V. (2014). Influence of nano-silica on the properties of recycled aggregate concrete. Construction and Building Materials, 55, 29-37. doi:10.1016/j.conbuildmat.2014.01.003.

[21] Ali, B., Qureshi, L. A., Shah, S. H. A., Rehman, S. U., Hussain, I., & Iqbal, M. (2020). A step towards durable, ductile and sustainable concrete: Simultaneous incorporation of recycled aggregates, glass fiber and fly ash. Construction and Building Materials, 251, 118980. doi:10.1016/j.conbuildmat.2020.118980.

[22] Katkhuda, H., & Shatarat, N. (2017). Improving the mechanical properties of recycled concrete aggregate using chopped basalt fibers and acid treatment. Construction and Building Materials, 140, 328–335. doi:10.1016/j.conbuildmat.2017.02.128.

[23] El Ouni, M. H., Shah, S. H. A., Ali, A., Muhammad, S., Mahmood, M. S., Ali, B., Marzouki, R., & Raza, A. (2022). Mechanical performance, water and chloride permeability of hybrid steel-polypropylene fiber-reinforced recycled aggregate concrete. Case Studies in Construction Materials, 16, 831. doi:10.1016/j.cscm.2021.e00831.

[24] Wang, Y., Hughes, P., Niu, H., & Fan, Y. (2019). A new method to improve the properties of recycled aggregate concrete: Composite addition of basalt fiber and nano-silica. Journal of Cleaner Production, 236, 117602. doi:10.1016/j.jclepro.2019.07.077.

[25] Shaban, W. M., Elbaz, K., Yang, J., Thomas, B. S., Shen, X., Li, L. H., Du, Y., Xie, J., & Li, L. (2021). Effect of pozzolan slurries on recycled aggregate concrete: Mechanical and durability performance. Construction and Building Materials, 276, 121940. doi:10.1016/j.conbuildmat.2020.121940.

[26] Xie, J., Huang, L., Guo, Y., Li, Z., Fang, C., Li, L., & Wang, J. (2018). Experimental study on the compressive and flexural behaviour of recycled aggregate concrete modified with silica fume and fibres. Construction and Building Materials, 178, 612–623. doi:10.1016/j.conbuildmat.2018.05.136.

[27] Ako, T. A., Onoduku, U. S., Oke, S. A., Essien, B. I., Idris, F. N., Umar, A. N., & Ahmed, A. A. (2014). Environmental effects of sand and gravel mining on land and soil in Luku, Minna, Niger State, North Central Nigeria. Journal of Geosciences and Geomatics, 2(2), 42–49. doi:10.12691/jgg-2-2-1.

[28] Mohamed, A. A. M. S., Al-Ajamee, M., Kobbail, A., Dahab, H., Abdo, M. M., & Alhassan, H. E. (2022). A study on soil stabilization for some tropical soils. Materials Today: Proceedings, 60, 87–92. doi:10.1016/j.matpr.2021.12.260.

[29] Behnood, A., Modiri Gharehveran, M., Gozali Asl, F., & Ameri, M. (2015). Effects of copper slag and recycled concrete aggregate on the properties of CIR mixes with bitumen emulsion, rice husk ash, Portland cement and fly ash. Construction and Building Materials, 96, 172–180. doi:10.1016/j.conbuildmat.2015.08.021.

[30] Omary, S., Ghorbel, E., & Wardeh, G. (2016). Relationships between recycled concrete aggregates characteristics and recycled aggregates concretes properties. Construction and Building Materials, 108, 163–174. doi:10.1016/j.conbuildmat.2016.01.042.

[31] Velenturf, A. P. M., Archer, S. A., Gomes, H. I., Christgen, B., Lag-Brotons, A. J., & Purnell, P. (2019). Circular economy and the matter of integrated resources. Science of the Total Environment, 689, 963–969. doi:10.1016/j.scitotenv.2019.06.449.

[32] Wang, B., Yan, L., Fu, Q., & Kasal, B. (2021). A Comprehensive Review on Recycled Aggregate and Recycled Aggregate Concrete. Resources, Conservation and Recycling, 171, 105565. doi:10.1016/j.resconrec.2021.105565.

[33] Verian, K. P., Ashraf, W., & Cao, Y. (2018). Properties of recycled concrete aggregate and their influence in new concrete production. Resources, Conservation and Recycling, 133, 30–49. doi:10.1016/j.resconrec.2018.02.005.

[34] Ajdukiewicz, A., & Kliszczewicz, A. (2002). Influence of recycled aggregates on mechanical properties of HS/HPC. Cement and Concrete Composites, 24(2), 269–279. doi:10.1016/S0958-9465(01)00012-9.

[35] Hansen, T. C., & Narud, H. (1983). Strength of Recycled Concrete Made From Crushed Concrete Coarse Aggregate. Concrete International, 5(1), 79–83.

[36] Ryu, J. S. (2002). An experimental study on the effect of recycled aggregate on concrete properties. Magazine of Concrete Research, 54(1), 7–12. doi:10.1680/macr.2002.54.1.7.

[37] Li, J. (2004). Study on mechanical behavior of recycled aggregate concrete. Master Thesis, Tongji University, Shanghai, China.

[38] Etxeberria, M., Vázquez, E., Marí, A., & Barra, M. (2007). Influence of amount of recycled coarse aggregates and production process on properties of recycled aggregate concrete. Cement and Concrete Research, 37(5), 735–742. doi:10.1016/j.cemconres.2007.02.002.

[39] Rahal, K. (2007). Mechanical properties of concrete with recycled coarse aggregate. Building and Environment, 42(1), 407–415. doi:10.1016/j.buildenv.2005.07.033.

[40] Evangelista, L., & De Brito, J. (2007). Mechanical behaviour of concrete made with fine recycled concrete aggregates. Cement and concrete composites, 29(5), 397-401. doi:10.1016/j.cemconcomp.2006.12.004.

[41] Khatib, J. M. (2005). Properties of concrete incorporating fine recycled aggregate. Cement and Concrete Research, 35(4), 763–769. doi:10.1016/j.cemconres.2004.06.017.

[42] Khoshkenari, A. G., Shafigh, P., Moghimi, M., & Mahmud, H. B. (2014). The role of 0–2mm fine recycled concrete aggregate on the compressive and splitting tensile strengths of recycled concrete aggregate concrete. Materials: Design, 64, 345–354. doi:10.1016/j.matdes.2014.07.048.

[43] Cabral, A. E. B., Schalch, V., Molin, D.C.C.D., & Ribeiro, J. L. D. (2010). Mechanical properties modeling of recycled aggregate concrete. Construction and Building Materials, 24(4), 421–430. doi:10.1016/j.conbuildmat.2009.10.011.

[44] Lovato, P. S., Possan, E., Molin, D.C.C.D., Masuero, Â. B., & Ribeiro, J. L. D. (2012). Modeling of mechanical properties and durability of recycled aggregate concretes. Construction and Building Materials, 26(1), 437–447. doi:10.1016/j.conbuildmat.2011.06.043.

[45] Younis, K. H., & Pilakoutas, K. (2013). Strength prediction model and methods for improving recycled aggregate concrete. Construction and Building Materials, 49, 688–701. doi:10.1016/j.conbuildmat.2013.09.003.

[46] Abbara, A. A., Abdelhalim, A., Al-Ajamee, M., Ahmed, O., Adhikary, S. K., & Ahmed, M. (2022). Uniaxial compressive stress-strain relationship for rubberized concrete with coarse aggregate replacement up to 100%. Case Studies in Construction Materials, 17, e01336. doi:10.1016/j.cscm.2022.e01336.

[47] Gelman, A., Carlin, J. B., Stern, H. S., & Rubin, D. B. (1995). Bayesian data analysis (1ST Ed.). Chapman and Hall/CRC, New York, United States. doi:10.1201/9780429258411.

[48] Kandiri, A., Sartipi, F., & Kioumarsi, M. (2021). Predicting compressive strength of concrete containing recycled aggregate using modified ann with different optimization algorithms. Applied Sciences (Switzerland), 11(2), 1–19. doi:10.3390/app11020485.

[49] Duan, Z. H., Kou, S. C., & Poon, C. S. (2013). Prediction of compressive strength of recycled aggregate concrete using artificial neural networks. Construction and Building Materials, 40, 1200–1206. doi:10.1016/j.conbuildmat.2012.04.063.

[50] Deshpande, N., Londhe, S., & Kulkarni, S. (2014). Modeling compressive strength of recycled aggregate concrete by Artificial Neural Network, Model Tree and Non-linear Regression. International Journal of Sustainable Built Environment, 3(2), 187–198. doi:10.1016/j.ijsbe.2014.12.002.

[51] Iqbal, M. F., Javed, M. F., Rauf, M., Azim, I., Ashraf, M., Yang, J., & Liu, Q. F. (2021). Sustainable utilization of foundry waste: Forecasting mechanical properties of foundry sand based concrete using multi-expression programming. Science of the Total Environment, 780, 146524. doi:10.1016/j.scitotenv.2021.146524.

[52] Naderpour, H., & Mirrashid, M. (2020). Estimating the compressive strength of eco-friendly concrete incorporating recycled coarse aggregate using neuro-fuzzy approach. Journal of Cleaner Production, 265, 121886. doi:10.1016/j.jclepro.2020.121886.

[53] Bu, L., Du, G., & Hou, Q. (2021). Prediction of the compressive strength of recycled aggregate concrete based on artificial neural network. Materials, 14(14), 3921. doi:10.3390/ma14143921.

[54] Onyelowe, K. C., Ebid, A. M., Riofrio, A., Baykara, H., Soleymani, A., Mahdi, H. A., Jahangir, H., & Ibe, K. (2022). Multi-Objective Prediction of the Mechanical Properties and Environmental Impact Appraisals of Self-Healing Concrete for Sustainable Structures. Sustainability, 14(15), 9573. doi:10.3390/su14159573.

[55] Zurada, J. (1992). Introduction to artificial neural systems. West Publishing Co, Eagan, United States.

[56] Alavi, A. H., & Gandomi, A. H. (2011). Prediction of principal ground-motion parameters using a hybrid method coupling artificial neural networks and simulated annealing. Computers and Structures, 89(23–24), 2176–2194. doi:10.1016/j.compstruc.2011.08.019.

[57] Rumelhart D. E, & McClelland J. L (1986) Parallel distributed processing, vol. 1: Foundations. MIT Press, Cambridge, United States.

[58] McClelland, J. L., & Rumelhart, D. E. (1989). Explorations in Parallel Distributed Processing - Macintosh version: A Handbook of models, Programs, and Exercises. MIT Press, Cambridge, United States. doi:10.7551/mitpress/5617.001.0001.

[59] Alavi, A. H., Gandomi, A. H., Mollahassani, A., Heshmati, A. A., & Rashed, A. (2010). Modeling of maximum dry density and optimum moisture content of stabilized soil using artificial neural networks. Journal of Plant Nutrition and Soil Science, 173(3), 368–379. doi:10.1002/jpln.200800233.

[60] Mollahasani, A., Alavi, A. H., Gandomi, A. H., & Rashed, A. (2011). Nonlinear neural-based modeling of soil cohesion intercept. KSCE Journal of Civil Engineering, 15(5), 831–840. doi:10.1007/s12205-011-1154-4.

[61] Dutta, R. K., Gnananandarao, T., & Ladol, S. (2020). Soft computing based prediction of friction angle of clay. Archives of Materials Science and Engineering, 104(2), 58–65. doi:10.5604/01.3001.0014.4895.

[62] Onyelowe, K. C., Ebid, A. M., Egwu, U., Onyia, M. E., Onah, H. N., Nwobia, L. I., Onwughara, I., & Firoozi, A. A. (2022). Erodibility of Nanocomposite-Improved Unsaturated Soil Using Genetic Programming, Artificial Neural Networks, and Evolutionary Polynomial Regression Techniques. Sustainability, 14(12), 7403. doi:10.3390/su14127403.

[63] Gnananandarao, T., Kumar Dutta, R., Khatri, V.N. (2021). Tsunamigenic Seismic Activity (Earthquakes) Prediction from III-Component Seismic Data. Seismic Hazards and Risk, Lecture Notes in Civil Engineering, 116. Springer, Singapore. doi:10.1007/978-981-15-9976-7_31.

[64] Gnananandarao, T., Dutta, R.K., Khatri, V.N. (2019). Application of Artificial Neural Network to Predict the Settlement of Shallow Foundations on Cohesionless Soils. Geotechnical Applications. Lecture Notes in Civil Engineering, 13. Springer, Singapore. doi:10.1007/978-981-13-0368-5_6.

[65] Dutta, R. K., Dutta, K., & Jeevanandham, S. (2015). Prediction of Deviator Stress of Sand Reinforced with Waste Plastic Strips Using Neural Network. International Journal of Geosynthetics and Ground Engineering, 1(2), 1–12. doi:10.1007/s40891-015-0013-7.

[66] Gnananandarao, T., Khatri, V. N., & Dutta, R. K. (2020). Prediction of bearing capacity of H shaped skirted footings on sand using soft computing techniques. Archives of Materials Science and Engineering, 103(2), 62–74. doi:10.5604/01.3001.0014.3356.

[67] Goh, A. T. C., Kulhawy, F. H., & Chua, C. G. (2005). Bayesian Neural Network Analysis of Undrained Side Resistance of Drilled Shafts. Journal of Geotechnical and Geoenvironmental Engineering, 131(1), 84–93. doi:10.1061/(asce)1090-0241(2005)131:1(84).

[68] Smith, G. N. (1986). Probability and statistics in civil engineering. Collins professional and technical books, New York City, United States.

[69] Garson, D. G. (1991). Interpreting neural network connection weights. AI EXPERT, 6(7), 47-51.

[70] Olden, J. D., & Jackson, D. A. (2002). Illuminating the "Black Box": A randomization approach for understanding variable contributions in artificial neural networks. Ecological Modelling, 154(1–2), 135–150. doi:10.1016/S0304-3800(02)00064-9.